

## Coherent Phonon Detection from Ultrafast Surface Vibrations

O. B. Wright and K. Kawashima

*Electronics Research Laboratories, Nippon Steel Corporation, 5-10-1 Fuchinobe, Sagamihara, Kanagawa 229, Japan*  
(Received 29 June 1992)

Using an optical technique, ultrafast vibrations of the surface of thin opaque films in the 0.1-THz range have been directly observed in the time domain. We propose a new type of phonon detection by monitoring the surface velocity, and demonstrate an exceptional sensitivity to atomic-scale inhomogeneities by observing an anomalous reflection from a buried film of monolayer order in thickness.

PACS numbers: 63.20.-e, 42.65.Re, 65.70.+y

The development of high-frequency monochromatic or broadband phonon excitation or detection techniques, such as those using thin-film superconducting tunnel junctions, heat pulses, or phonon-induced fluorescence, provided the initial stimulus for terahertz phonon propagation and spectroscopy studies in bulk solids [1]. To avoid the need for low temperatures or high vacuum or for deposited films which reduce efficiency and distort phonon pulse shapes, purely optical methods have also played an important role. For example, Raman or Brillouin scattering in the time or frequency domains can, in addition, probe the vibrational properties of thin or ultrathin films, but are usually limited to acoustic phonon frequencies below  $\sim 0.1$  THz because of wave-vector conservation. More recently, with time-resolved picosecond or femtosecond optical pump and probe methods [2-5] acoustic or optical phonons are detected through photoelastic or electro-optic effects, respectively.

Given that a phonon represents a quantum of lattice vibration, it is natural to imagine what could be considered as the most direct phonon detection method: the time-resolved measurement of atomic or molecular vibration amplitude. To our knowledge there has been no report of this type of high-frequency ( $\sim 0.1$  THz) phonon detection at an opaque surface, the previous highest frequencies being on the order of 2 to 5 GHz with the optical pump-probe technique combined either with laser-induced gratings [6] or with laser beam deflection [7]. We recently reported the detection of picosecond vibrations of transparent films using time-resolved interferometry [8]. However, the reflectance change caused by surface motion is obscured by a signal arising from the photoelastic effect that prevents resolution of the phonon pulse shape. Similarly, with the picosecond time-resolved reflectivity method [2,4], the detected pulse shapes are distorted by optical penetration and depend on (often unknown) photoelastic constants of the film. These problems have, for example, hindered the investigation of the processes involved in phonon generation with picosecond light pulses [2].

Motivated by the success of photothermal deflection measurements of transient thermal expansion and surface waves in the MHz to GHz range [6,7,9], we extend such measurements up to  $\sim 0.2$  THz with polycrystalline films of the group-VI transition metals molybdenum and

chromium, report the *essentially undistorted* detection in these materials of coherent longitudinal acoustic phonon pulses, and show how the phonon frequency spectrum can be obtained.

The apparatus used is that of Rothenberg [7]. Phonons are excited by a laser pump pulse (energy 0.4 nJ) and surface vibrations are interrogated through changes in surface slope  $\psi$  by a weaker (0.02 nJ) probe pulse of perpendicular ( $s$ ) polarization, which is angularly deflected by  $\delta\theta = 2\psi$ . The output of a mode-locked dye laser with a photon energy of 2 eV ( $\lambda = 630$  nm), pulse duration 2 ps (FWHM), and repetition rate 76 MHz is split to obtain these pulses. The pump beam, chopped at 5 MHz for in-phase synchronous detection, is focused at  $20^\circ$  incidence to a  $15\text{-}\mu\text{m}$ -diam spot. The probe beam, focused at  $\theta = 5^\circ$  incidence to a similar spot size, overlaps with the pump beam to give the maximum  $\delta\theta$ . The reflected probe beam is collimated onto a bicell detector to obtain  $\delta\theta(t)$ . Although the optical pulse duration used is twice that of Ref. [7], the phonon frequencies excited here are  $\sim 50$  times greater because of the larger optical absorption length ( $\zeta$ ) of the bulk silicon sample used in Ref. [7]. Our pulse duration ( $\Delta t$ ) is still sufficiently short ( $\Delta t < \zeta/v$ ,  $v$  the longitudinal sound velocity) for the excited phonon spectrum to be primarily determined by  $\zeta$  in our samples.

The maximum transient temperature changes are  $\sim 50$  K, which give rise to (outward) surface displacements  $\delta z \sim 0.003$  nm, with  $\delta\theta \sim 1$   $\mu\text{rad}$ . At 1-Hz bandwidth the resolution is 20 times below this (10 times smaller than in Ref. [7]), limited by laser intensity and beam-pointing fluctuations. For relative intensity changes, we have obtained (as other groups [2-4]) a resolution up to 10 times smaller than this [8], down to near the quantum noise limit, but the level for these first experiments is sufficient to detect the relatively weak signals for our samples.

We first tested the method with a 190-nm film of Mo, sputtered (rf magnetron at 20 nm/min) at room temperature on a silica substrate. Its thickness was determined from the acoustic echo times ( $v \approx 6440$   $\text{ms}^{-1}$ ) [10], and verified by needle profiling to  $\pm 10\%$ . We obtain clear resolution of echoes in Fig. 1(a) from multiple reflections of phonons inside the film. Their unipolar shape can be understood by using a one-dimensional thermoelastic model in the nondispersive acoustic near field [2]. Initial-

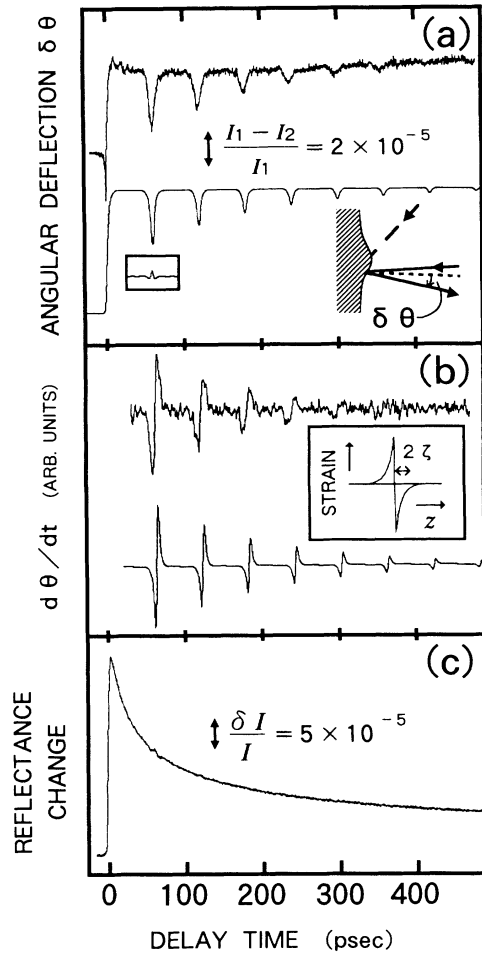


FIG. 1. Curves against pump-probe delay time for a 190-nm film of Mo on a silica substrate. (a) Upper curve: probe beam angular deflection  $\delta\theta$ . Lower curve: fit from thermoelastic model. The beam geometry and the photoelastic contribution to the first echo (inset with same scale) are shown. (b) Upper curve:  $d\theta/dt$ . Lower curve: theoretical fit. Inset: calculated strain pulse spatial profile for infinitely short optical pulses. (c) Reflectivity trace (with exact overlap of laser spots). Scales are given in terms of relative intensity changes. [ $I_1$  and  $I_2$  in (a) correspond to the two elements of the bicell detector.]

ly, strain ( $\sim 10^{-4}$ ) is induced within a depth ( $z$ ) on the order of  $\zeta$  ( $\approx 16$  nm by ellipsometry). The resulting longitudinal strain pulse, for times  $t \gg \zeta/v$  ( $\zeta/v \approx 2.5$  ps), is given by  $\eta_{33a}(T) = \eta_0 \text{sgn}(T) \exp(-|T|/\zeta)$ , as shown in the inset of Fig. 1(b) at a fixed time, where  $T = t - z/v$ . This pulse is composed of a broad range of frequencies, peaked at  $v/2\pi\zeta \approx 80$  GHz. The lower curve in Fig. 1(a) is evaluated from the total time-varying strain distribution,

$$\delta z(t) = \int_0^\infty \eta_{33}(z, t) dz,$$

including the smoothing effect of both the pump and probe pulse durations. The fit reproduces the echo shape and the effect of the initial thermal expansion. The ob-

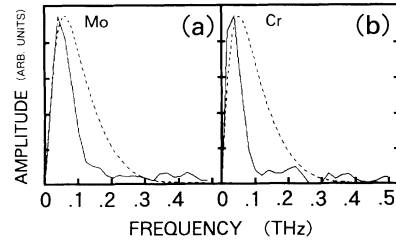


FIG. 2. Phonon pulse spectra compared to the predictions of the thermoelastic model (dashed curves), corresponding to (a) the first echo of the Mo film, and (b) echo from a Cr film [from Fig. 3(e)]. All fitted curves in this paper include the effect of the optical pump and probe pulse duration.

served negative step in  $\delta\theta$  near  $t=0$  is not caused by surface displacement. It can be attributed to the radial gradient of the near-surface dielectric constants caused by the transverse temperature distribution [7]. (We have not tried to model this thermal component. The absence of a decay in the average signal level may be due to a balance between this and the relaxing thermal expansion.) We neglect for the moment the effects of the strain-induced radial gradients of the dielectric constants on the echo shape.

In general, for the reflection of a longitudinal strain pulse at a free surface, the time dependence of the surface velocity  $V(t) = d(\delta z)/dt$  is identical to that of the incoming strain pulse [ $\eta_{33i}(t + z/v)$ ], assuming that the transverse spatial extent of the pulse is large compared to the acoustic wavelength ( $\sim 2\pi\zeta$  here):

$$V(t) = -2v\eta_{33i}(t).$$

The upper trace in Fig. 1(b) shows the data for  $d\theta/dt \propto V(t)$ , evaluated numerically. Apart from the smoothing caused by the optical probe pulse duration, the *phonon strain pulse shape is therefore directly obtained*. A similar shape is predicted by the thermoelastic model (lower curve).

The potential of our technique for phonon spectroscopy is now evident. The spectrum for an individual pulse can be evaluated by taking the Fourier transform of  $d\theta/dt$ , as shown in Fig. 2(a) for the first echo together with the thermoelastic model (dashed curve). This spectrum and the generated pulse shape are sensitive to the microscopic origin of the stress [2]. The nonequilibrium transfer of the electron excess energy to the phonons through electron-phonon collisions will broaden the strain pulse and narrow the frequency spectrum because the electrons may diffuse a significant distance (compared to  $\zeta$ ) before they lose their energy [11]. In addition the phonons diffuse by thermal conduction. An estimate of the latter effect [12] (according to the method of Ref. [2]) cannot explain the observed symmetric broadening by a factor of about 2 [Fig. 1(b)]. Our direct measurements of phonon strain therefore provide evidence for electron diffusion during pulse generation. Similar conclusions apply for Cr

[see Fig. 2(b)]. We have not tried to model the effect of diffusion processes on the pulse spectra.

The echo decay is well modeled using acoustic impedances from the literature [10]. For longer propagation distances, decay or broadening effects from acoustic attenuation, and, particularly at high frequencies, dispersion or anharmonicity may appreciably affect the phonon pulse shape.

For comparison, we have carried out time-resolved reflectivity measurements taken under identical conditions at the same point of the film, as shown in Fig. 1(c). The bipolar echo shape gives a distorted measure of the phonon strain because of the smearing effect from optical penetration into the film, which limits the resolution for detection to frequencies  $\lesssim 0.2$  THz for materials with  $\zeta \sim 20$  nm at visible wavelengths [13]. In contrast, the beam deflection detection, essentially local to the surface, is only limited by the optical pulse duration (to frequencies  $\lesssim 0.2$  THz here) and not by  $\zeta$ . This is one important advantage of our method. Another is the improvement in sensitivity by a factor of 6 in units of relative intensity modulation per unit strain [14]. The third stated advantage, that of the direct detection of the phonon strain pulse, can be justified by calculating the contribution to the beam deflection  $\delta\theta_g$  from the radial gradient of the strain. Extending Rothenberg's optical far-field analysis [7] for depth-independent changes to our time and depth-dependent case, we obtain

$$\frac{\delta\theta_g(t)}{\delta\theta_{\max}} = \frac{\kappa}{4\eta_0} \frac{\delta\bar{R}(t)}{R}, \quad (1)$$

where  $\delta\theta_{\max}$  is the maximum change in  $\delta\theta$  (for the echo considered) owing to surface vibration,  $\delta R(dn/d\eta, d\kappa/d\eta, \dots)$  the expression ( $\propto \eta_0$ ) for reflectance change derived by Thomsen *et al.* [2],  $\delta\bar{R}(t) = \delta R(d\kappa/d\eta, -dn/d\eta, \dots)$ ,  $\eta_0$  the incident strain amplitude, and  $n + i\kappa$  the refractive index ( $= 2.9 + 3.2i$ ). The prediction of Eq. (1) for the first echo is shown in the Fig. 1(a) inset. At its peak value  $\delta\theta_g$  represents only 15% of the signal. In addition, the actual *distortion* of the strain pulse shape (and hence the spectrum) is half this amount, on the order of the noise level. We have therefore neglected this contribution. In evaluating Eq. (1) we used approximate values of the photoelastic constants [15] derived by quantitative fitting of the signal amplitude in Fig. 1(c). Similar values were found for Cr, and we apply the same approximations for this material.

We have also observed echoes in films of aluminum and amorphous silicon. For the former the photoelastic contribution was estimated to be approximately 40%, whereas for the latter it is completely negligible. Both the photoelastic and thermoreflectance constants of metals and semiconductors are strongly wavelength dependent in the visible where phonon energies coincide with interband transition energies [16]. It should be possible in general to tune the excitation wavelength to minimize the photoelastic contribution to the echoes, and thereby

broaden the application of the method to a wider variety of materials.

High-frequency phonons are scattered by atomic-scale defects such as dislocations, grain boundaries, voids, isotopes, or disorder [11]. As an example of a structure with such a defect, we prepared a series of ultrathin layers of *a*-Si buried under Cr (chosen for large acoustic mismatch): a 330-nm Cr base film, the *a*-Si layer, and a 670-nm Cr top layer were sputtered on silica substrates, maintaining vacuum conditions throughout. Thicknesses were calculated from deposition times [30 and 50 min for  $1 \mu\text{m}$  ( $\pm 5\%$ ) calibration films of Cr and *a*-Si]. Results for a film of *a*-Si of thickness  $L = 16$  nm are shown in Fig. 3(a), with the thermal background subtracted in Fig. 3(b). The two echoes correspond to phonon reflection from the thin layer and from the substrate. The phonon pulse shape is changed on reflection from this layer, and is also slightly distorted on transmission (owing to multiple reflections). The lower curves show the pulse shapes based as before on the thermoelastic model and continuum acoustics ( $v = 8100 \text{ m s}^{-1}$  for *a*-Si from separate ex-

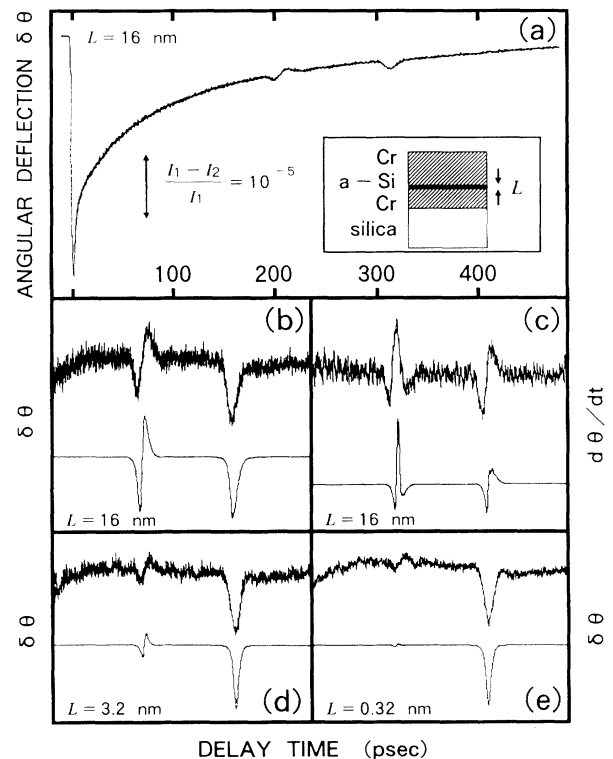


FIG. 3. Experimental curves against pump-probe delay time and theoretical fits according to thermoelastic theory for a series of three-layer film structures containing an ultrathin *a*-Si film (see inset). (a) Probe beam angular deflection  $\delta\theta$  for a 16-nm *a*-Si film. (b) Upper curve: data of (a) with background subtracted. Lower curve: theoretical fit. (c) Upper curve:  $d\theta/dt$  for the 16-nm *a*-Si film. Lower curve: theoretical fit. (d), (e) The data and fits for the 3.2- and 0.32-nm films of *a*-Si.

periments and  $\zeta=17$  nm [8]) including multiple reflections up to order 7. Good correlation is obtained, both for  $\theta$  and for  $d\theta/dt$  [Fig. 3(c)]. (For a thin layer the acoustic reflection coefficient is proportional to  $i\omega L$ ,  $\omega$  the angular frequency, giving a reflected pulse shape  $\propto Ld\eta_{33i}/dt$ .)

We also investigated *a*-Si films of statistical thicknesses 3.2 and 0.32 nm, the latter of order 2 monolayers (by comparison with crystalline Si for the [100] orientation). Data (checked to be independent of the measurement position on the film surface) and fits for  $\delta\theta$  ( $\propto \delta z$ ) are shown in Figs. 3(d) and 3(e). The *a*-Si echo from the 0.32-nm film is significantly larger than the prediction of continuum acoustics. This striking finding is in qualitative agreement with lattice dynamical simulations of specular phonon reflection from a buried, crystalline atomic monolayer [17]. However, like similar anomalies observed for phonons diffusely reflected at solid-solid interfaces in low-temperature phonon pulse or thermal transport experiments [1,18], disorder or strain at the interfaces, where there is a large lattice mismatch, or island formation could be the main cause. Although we cannot yet distinguish the precise mechanisms responsible, our experiments point the way to comparative investigations with more characterized samples, perhaps using epitaxial semiconductor films or metal-metal interfaces, to study directly their lattice dynamics by monitoring the phonon strain in the time domain. One application is the probing of interfacial strain in multilayer compositionally modulated metal films, which is thought to be responsible for their anomalous elastic properties [19].

In conclusion, we have directly observed the time-resolved motion of opaque surfaces in the 0.1-THz region for the first time and have shown how phonon pulses may be thereby detected. In the group-VI transition metals studied, resolution of the phonon strain pulse shape and spectrum is possible, and comparison with available models provides a detailed probe for the electron-phonon dynamics of the phonon pulse generation. In addition, the observation of anomalous reflections from ultrathin films with this method—in essence a real-time experiment in lattice dynamics on an atomic scale—will lead to a greater understanding of the physics of bonding and interfacial strain. Many other exciting extensions and applications can be envisaged. The potential for extension to higher frequencies, conceivably up to the Brillouin-zone edge, could be exploited to probe, for example, the normal modes of semiconductor heterostructures or phonon localization in amorphous materials.

We thank Dr. W. A. Phillips and Dr. G. Fasol for fruitful discussions.

[1] W. E. Bron, Rep. Prog. Phys. **43**, 301 (1980); M. N. Wy-

- bourne and J. K. Wigmore, Rep. Prog. Phys. **51**, 923 (1988).
- [2] C. Thomsen, H. T. Grahn, H. J. Maris, and J. Tauc, Phys. Rev. B **34**, 4129 (1986).
- [3] C. Thomsen, H. T. Grahn, H. J. Maris, and J. Tauc, Opt. Commun. **60**, 55 (1986).
- [4] G. L. Eesley, B. M. Clemens, and C. A. Paddock, Appl. Phys. Lett. **50**, 717 (1987).
- [5] G. C. Cho, W. Kutt, and H. Kurz, Phys. Rev. Lett. **65**, 764 (1990); K. P. Cheung and D. H. Auston, Phys. Rev. Lett. **55**, 2152 (1985).
- [6] J. J. Kasinski, L. Gomez-Jahn, K. J. Leong, S. M. Graecwski, and R. J. Dwayne Miller, Opt. Lett. **13**, 710 (1988).
- [7] J. E. Rothenberg, Opt. Lett. **13**, 713 (1988).
- [8] O. B. Wright, J. Appl. Phys. **71**, 1617 (1992); O. B. Wright and T. Hyoguchi, Opt. Lett. **16**, 1529 (1991).
- [9] J. Opsal, A. Rosencwaig, and D. L. Willenborg, Appl. Opt. **22**, 3169 (1983).
- [10] J. A. Bell, R. Zanoni, C. T. Seaton, G. I. Stegeman, J. Makous, and C. M. Falco, Appl. Phys. Lett. **52**, 610 (1988).
- [11] M. I. Kaganov, I. M. Lifshitz, and L. V. Tantarov, Zh. Eksp. Teor. Fiz. **31**, 2232 (1956) [Sov. Phys. JETP **4**, 173 (1957)]; S. I. Anisimov, B. L. Kapeliovich, and T. L. Perelman, Zh. Eksp. Teor. Fiz. **66**, 776 (1974) [Sov. Phys. JETP **39**, 375 (1975)].
- [12] The effect of thermal diffusion depends on the parameter  $D/v\zeta \approx 0.05$  for our Mo film, with the thermal diffusivity  $D$  calculated from the data of Fig. 1(c) using the method of C. A. Paddock and G. L. Eesley, J. Appl. Phys. **60**, 285 (1986), ignoring electron diffusion. This changes the strain pulse asymmetrically, slightly broadening only the trailing side (see Ref. [2]). We assume the *a*-Si film does not affect the substrate echo in Fig. 3(e).
- [13] Higher frequencies up to  $\sim 0.5$  THz using overlaid thin transducer films are possible. See, for example, T. H. Zhu, H. J. Maris, and J. Tauc, Phys. Rev. B **44**, 4281 (1991). This further distorts the phonon pulse shapes.
- [14] An enhancement of order 10 is predicted by using a simple model for the maximum angular deflection,  $\delta\theta_{\max} \approx \eta_0\zeta/w$ ,  $w$  the spot size, and the associated relative intensity change,  $(I_1 - I_2)/I_1 \approx w\delta\theta/\lambda$ ; the expression for  $\delta R/R$  is taken from Ref. [2].
- [15] We find  $dn/d\eta = dk/d\eta \approx -0.5$ , taking account of the Gaussian profile of the pump and probe beams and the pulse duration. An independent estimate is possible using the method of Ref. [8] and, for the case of Cr for which results are available, consistent values ( $|dn/d\eta| < 1$  and  $|dk/d\eta| < 1$ ) are obtained.
- [16] M. Cardona, *Modulation Spectroscopy* (Academic, New York, 1969), Chaps. 5 and 6.
- [17] B. V. Paranjape, N. Arimitsu, and E. S. Krebes, J. Appl. Phys. **61**, 888 (1987).
- [18] E. T. Swartz and R. O. Pohl, Rev. Mod. Phys. **61**, 605 (1989).
- [19] B. M. Clemens and G. L. Eesley, Phys. Rev. Lett. **61**, 2356 (1988).